Ultimate bond strength assessment of uncorroded and corroded reinforced recycled aggregate concretes

Ignasi Fernandez[1], Miren Etxeberria*[1], Antonio R. Marí[1]

[1] Department of Construction Engineering, Polytechnic University of Catalonia, Jordi Girona, 1-3, Barcelona 08034, Spain.

*corresponding author. Telephone: +34 934011788, email: miren.etxeberria@upc.edu

Keywords:

steel reinforced concrete; modelling studies; rust

Abstract:

This experimental study assesses the bond performance of recycled aggregate concretes (RAC) with embedded uncorroded and corroded steel bars. The RAC were produced using 20%, 50% and 100% of coarse recycled aggregates obtained from the crushing of waste 40 MPa compressive strength concrete. Three degrees of corrosion were reached on the steel bars. The uncorroded RAC specimens presented a comparable bond strength to that of conventional concrete (CC). Low corroded RAC specimens presented better bond performance and later superficial cracking when compared to those of CC. At a higher corrosion degree, all concretes presented a similar bond capacity. The ultimate bond strength estimation models used for CC were adequate for its prediction on RAC.

1. Introduction

Corrosion of the steel bars is one of today's most frequent and significant type of damage, in existing reinforced concrete structures. Therefore, the study of the structural effects of bars corrosion is crucial in determining the structural performance and residual strength of impaired structures. One of the most severe reinforcement corrosion effects is the change in bond properties between steel and concrete. Moreover, volumetric expansion of corrosion products causes serious problems by inducing splitting stresses along corroded reinforcement, with possible resulting damage to the surrounding material. Generally, the splitting stresses are not tolerated by concrete, resulting in cracking and eventually spalling of the cover. As the reinforcement becomes more exposed, the corrosion rate may increase and facilitate the deterioration process.

Steel reinforcement unconfinement due to cover cracking or spalling of concrete cover, as well as rust between both materials, quickly decreases the bond strength, thus changing the structural behaviour and inducing anchorage failures. Many researchers have extensively studied the effect of the corrosion process on bond deterioration extensively. Several studies have dealt with the investigation of the parameters that may influence the bond and anchorage capacity of corroded structures [1–5]. Models studying the interaction between both materials, and numerous experimental studies identifying and studying this phenomenon can be found in the literature on the subject [6–9]. Even though, the literature on works covering bond behaviour on recycled aggregates is very sparse [10–17].

The increasing amount of construction wastes coming from old and deteriorated structures at the end of their service life has a relevant environmental impact on the construction sector as the results of the economic benefits of using the wastes produced in the form of

recycled concrete aggregates (RCA) in the concrete employed in reinforced concrete production. Wastes from older structures yield fragments in which the aggregate is contaminated with various different substances such as gypsum, asphalt, etc. A proper treatment of the recycled aggregate, as well as an accurate production process, results in recycled aggregate concrete (RAC) being a very suitable option to reduce the overall cost in the construction sector [18]. Over the past 50 years, the use of RCA has been profoundly studied for concrete production [18–27] and the resulting studies maintain that the primary weakness of RCA is its high porosity, which could directly influence a decrease in the compressive strength and durability of concretes produced with those aggregates.

Recent studies have tried to determine the bond between both the RAC and the steel with respect to that of conventional concrete (CC) and steel [13]. These studies manifest that a reduction of bond strength could be associated with the amount of recycled aggregate used in the mixture. Several authors [13,15,16] reported reductions of 6-8% up to 30% of bond capacity, nevertheless other researchers' work [10] noted differences of approximately 1% of the bond strength of recycled aggregate concrete with respect to that of CC concrete. Although the reduction in bond strength is strongly related to the concrete's compressive strength, it is also dependent on other parameters such as steel bar rib geometry and the position and orientation of the bars during casting. The amount of concrete cover also has an important influence on this phenomenon [10,28–33].

In this experimental study of the bond strength and bond behaviour between recycled aggregate concrete and reinforcement steel, either corroded or uncorroded, using the direct pull-out tests was presented. Two experimental phases were conducted, one with uncorroded and another with corroded steel bars embedded in RAC and CC concrete cube

specimens. For that purpose, four different concrete mixtures were cast in each phase by replacing 0% (using 100% of natural aggregates, CC concrete), 20% (RAC-20), 50% (RAC-50) and 100% (RAC-100) of natural coarse aggregates for coarse recycled concrete aggregates. The obtained results for RAC concretes were compared with the results obtained from the CC concrete, before finally being compared to other models encountered in the literature referring to the bond strength capacity of reinforced conventional and recycled concrete.

2. Materials

2.1 Materials

Type I Portland cement, CEM I 42.5R, was used in concrete mixtures with rapid hardening and 42.5 MPa characteristic strength cement. The chemical properties of cement are given in Table 1.

Table 1. Chemical composition of cement

Composition	SiO_2	Fe_2O_3	Al_2O_3	CaO	MgO	K_2O	Na_2O	SO_3	LOI
%	19.16	3.56	5.04	62.9	1.66	0.75	0.15	3.54	3.25

Natural limestone, fine (FA, 0/4 mm) and coarse aggregates (two fractions; CA1 of 4/12 mm and CA2 fraction of 12/20 mm) were used for concrete production. Physical properties, density and absorption, and the grading distributions are described in Table 2 and Fig. 1, respectively. The properties of the fine and coarse aggregates were determined according to EN specifications. All fractions of natural aggregates satisfy the requirements specified by the Spanish Standard of Structural Concrete [34].

RCA aggregates were obtained by crushing rejected 40 MPa compressive strength concrete produced by a precast concrete company. The properties of RCA of density, absorption and grading size are shown in Table 2 and Fig. 1, respectively. It was found that the density of RCA was found to be lower than that of the natural aggregates and the absorption capacity was higher. The porosity of RCA determined by mercury Intrusion porosimetry (MIP) was 8.63% and its average pore diameter was 0.048 μm. The grading was defined by 4/20 mm, which complied with the Spanish Standard of Structural concrete regulations [34] in its employment for recycled concrete production and it was used in substitution of CA1 and CA2 natural coarse aggregates.

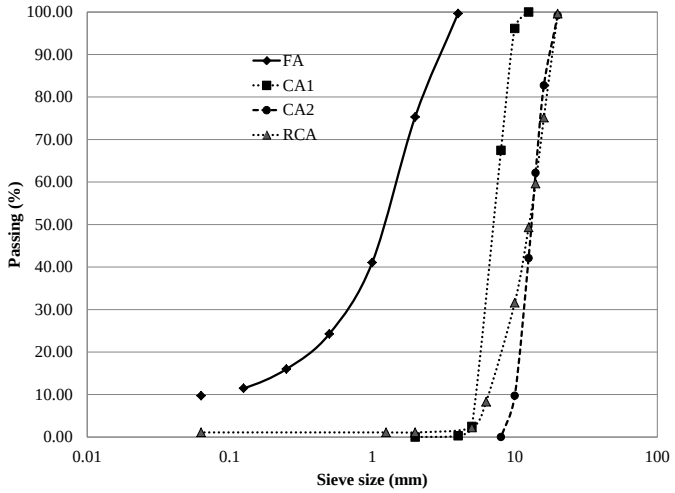

Fig. 1. Grading distribution of fine natural aggregates (FA) and coarse natural (CA1 and CA2) and recycled aggregates (RCA)

Table 2. Dry density and water absorption capacity of aggregates

Properties	CA2 12/20mm	CA1 4/12mm	FA 0/4mm	RCA
Dry density (kg/dm^3)	2.65	2.64	2.58	2.30
Water absorption (%)	0.67	0.87	1.68	5.91

101 At concrete production 4% NaCl in weight of cement was added to the mixture; the aim of
102 which was the depassivation of the steel inside the concrete and the causing of a conductive
103 medium to facilitate the corrosion procedure. Superplasticizer was also used to provide the
104 desired workability of the mixture.

105 *2.2 Concrete mix proportions*

106 The four mixtures (Conventional concrete, CC; concrete produced with 20% of RCA,
107 RAC-20; concrete produced with 50% of RCA, RAC-50; concrete produced with 100% of
108 RCA, RAC-100) were prepared and cast. The replacement of raw, coarse aggregates for
109 recycled coarse aggregates was carried out according to the volume.

110 The mix proportion of CC concrete was defined with 300kg of cement and a total water-
111 cement ratio of 0.5 for concretes exposed to a marine and chloride environment as
112 described by the Spanish Structural Concrete code [34]. The effective water-cement ratio of
113 CC concrete was determined and maintained constant in all RAC concretes. The total w/c
114 ratio of RAC was higher than for CC, due to higher absorption capacity of RCA[24].

115 It is taken as understood that the effective water / cement ratio of the concretes is the ratio
116 between the effective water (free water which reacts with cement) and total cement weight.
117 The effective water was determined by first calculating the total water used for concrete
118 production and then subtracting both the water absorbed by the aggregates and the moisture
119 present in RCA during concrete production. The previously mentioned water amount
120 absorbed by aggregates at concrete production is termed as the effective water absorption
121 capacity of aggregates and it was determined experimentally. The experiment consisted of
122 submerging the aggregates in water for 20 minutes [24]. The effective water absorption

123 capacity of natural coarse and fine aggregates was 20% and 80% of their total water
124 absorption capacity, respectively. The recycled aggregates had an effective water
125 absorption capacity of 70% of their total capacity. (The total water absorption capacity of
126 the aggregates is described in Table 2). The effective w/c ratio on CC concrete was
127 approximately 0.45 and it mantained constant in all RAC concretes.

128 The control of the effective water/cement ratio in the production process of recycled
129 aggregate concrete can only be obtained by using recycled aggregates with aproximately a
130 moisture level of between 80%-90% of their total absorption capacity [24] (in order to
131 reduce their total absorption capacity [26]). The coarse recycled concrete aggregates were
132 wetted the day before use via a sprinkler system and then covered with a plastic sheet so as
133 to maintain their humidity (aprox. at 80% of their absorption capacity) until used in
134 concrete production. During concrete production, recycled aggregates absorbed a certain
135 amount of free water due to their initial moderate moisture content. This effectively lowers
136 their w/c ratio in the interfacial transition zone (ITZ), consequently improving the
137 interfacial bond between the aggregates and cement [27]. It is well known that the
138 compressive strength of concrete made with saturated aggregate is lower than concrete
139 made with air dried aggregates due to the adverse effect of the bleeding of the saturated
140 aggregates [23].

141 Concrete mix proportions were defined according to their maximum volumetric
142 compaction. This mix proportion for conventional concrete (CC) was defined as 50% of
143 fine aggregates and 50% of coarse aggregate. The distribution of coarse aggregate was 30%
144 CA1 4/12mm and 70% of CA2 12/20mm. The same volume of CA1 and CA2 was
145 replaced by RCA for each recycled aggregate concrete production.

Table 3 shows the mix proportions used. The weight of aggregates is given as their dry weight. The total amount of water was considered, including the effective absorbed water by aggregates as well as the 80-90% of humidity of recycled aggregates at concrete production. 4% of NaCl and 1% of superplasticizer were used in all concretes with respect to cement weight.

Table 3. Mix proportions of the concretes mixtures

Material (1000 litres)	CC	RCA-20	RCA-50	RCA-100
Cement (kg)	300	300	300	300
Total Water (kg)	150	159	172	194
Effective w/c	0.45	0.45	0.45	0.45
FA 0/4mm	976	976	976	976
CA1 4/12mm	210	168	105	-
CA2 12/20mm	765	612	383	-
RCA	-	171	428	855
NaCl (weight of cement)	4%	4%	4%	4%
Superplasticizer (weight of cement)	1%	1%	1%	1%

3 Experimental campaign and test procedure

The concrete compressive strength was determined for all concrete types. Bond strength between concrete and steel bars both corroded and uncorroded were analysed by means of two experimental phases.

3.1 Compression test

The compressive strength of concrete was determined using a compression machine with a loading capacity of 3000 kN. The compressive strength was measured at the age of 28 days following UNE-EN 12390-3 specifications. Three cylindrical specimens (100mm of diameter and 200 mm of length) were used for each type of concrete produced.

3.2 Pull-out test

The experimental work presented here focuses on the direct pull-out test of both the natural aggregate concrete, and the recycled aggregate concretes, reinforced with steel bars. The underlying purpose of the work focusing on the characterization of the corresponding bond behaviour. Pull-out test is a widely used test employed to obtain the local bond behaviour for short embedded length steel specimens. The typical assumption for short pull-out tests with ribbed steel reinforcement bars, defined by embedment length of less than five times the bar diameter, is that the distribution of bond stresses is uniform along the bonded section [35,36]. Accordingly, the hypothesis of the uniform bond stresses was assumed and the local bond stress could be estimated as:

$$\tau = P / \pi \Phi L \quad (1)$$

where, P is the applied load, Φ is the nominal diameter of the steel bar, and L is the embedded length.

The experimental study was divided into two phases. In experimental Phase 1 the test was performed according to the code recommendations [37]. In experimental Phase 2, some concrete specimens were summited to accelerated corrosion and consequently the embedded bar design was modified with respect to the criteria defined by the code. The pull-out test were carried out through the use of 100x100 mm cubic specimens which had embedded steel in the upper face. For the purpose of this study the top, bottom and sides of the concrete cube shall be known as upper face, bottom face and lateral faces.

3.2.1 Pull-out test: Phase 1

The experimental setup was conducted following the code recommendations [37] and using a specific fatigue machine INSTRON 8800.

Steel bars of ϕ12 mm were embedded in the centre of the 100x100 mm cubic concrete specimens. The steel bars completely crossed the cube section of 100 mm. A piece of plastic tube was used to debond 50 mm of the steel bar from the concrete, leaving the other 50 mm to bond with the concrete (see Fig. 2a). In total 16 cubic specimens were cast, four for each concrete type.

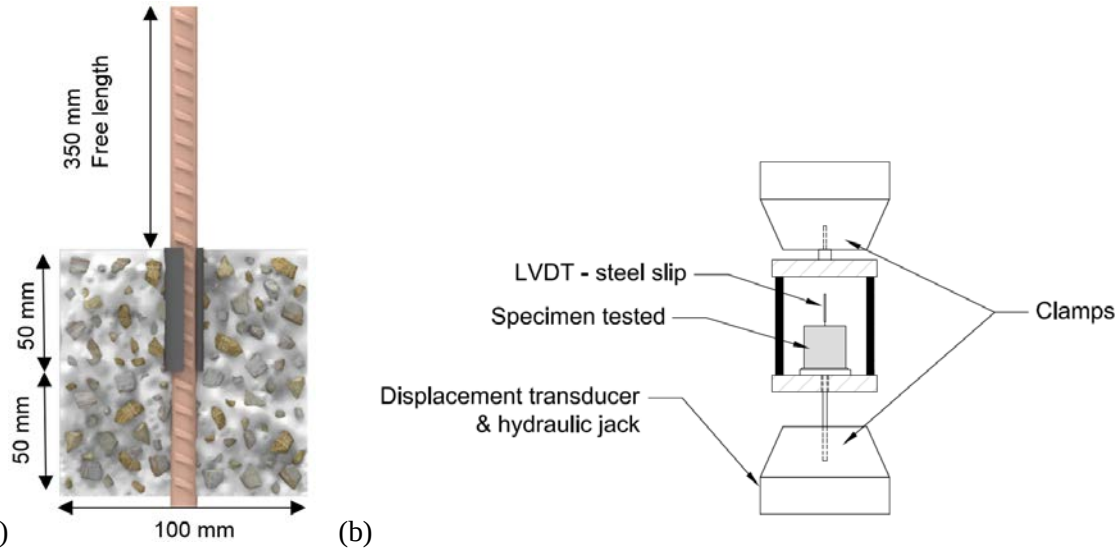

Fig. 2. (a) Concrete specimen description (phase 1) (b) Test setup, direct pull-out test

The total slip between both the concrete and the steel was measured during the test. An LVDT was affixed to the concrete cube at the specimen's bottom in order to register the total rebar slip.

The hydraulic jack clamps were attached to the steel bar-end. The load was applied directly to the bar by means of control displacement, in order to achieve results on both the pre and post peak behaviour up to failure, as well as the residual bond capacity. The applied load

198 and the LVDT readings were recorded every half a second by means of a DAQ. The test
199 was conducted using a constant velocity of 0.2 mm/min. Fig. 2b shows the experimental
200 setup.

201 *3.2.2 Pull-out test: Phase 2*

202 The Phase 2 test specimen design was modified with respect to that defined by the code
203 [37]. The reason for this modification was to facilitate a simpler and more reliable method
204 of the steel corrosion procedure. 16 cubic specimens of 100 mm were cast for each
205 designed concretes. ϕ10 mm steel bar diameter were used in the experimental Phase 2 and
206 the bars, as Fig. 3 shows, did not fully cross the whole concrete section of 100 mm. The
207 free steel length for all the specimens, was 350 mm and the bonded section was 50 mm.

208 The bars were embedded from the centre of the upper surface of the cubic specimens to a
209 length which was equivalent to five times that of the steel bar diameter. The moulds used
210 were specially designed in order to ensure that the bars were fixed at the same position in
211 all the specimens. Fig. 3 describes the test specimens and the established setup. 45 mm of
212 concrete covered the embedded bar in all directions. This configuration ensured the same
213 corrosion degree guaranteed in all the embedded section of the steel bar.

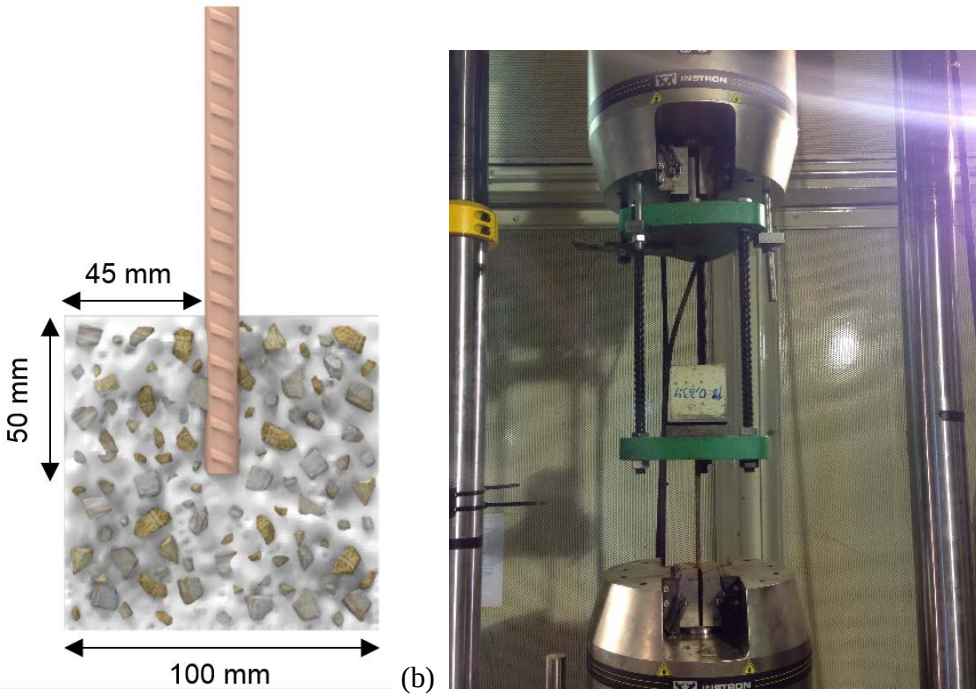

Fig. 3. (a) Concrete specimen description (Phase 2) (b) Pull-out test setup

In this study case hydraulic jack clamps also were attached to the steel bar-end in order to pull the bar out of the concrete. The tests were conducted by means of displacement control, of 0.2 mm/min, until failure or until the residual bond load was reached.

The load was applied directly to the bar via a hydraulic jack controlled by a load cell. The total displacement, as well as the applied load, were registered. Each measurement was recorded and stored every half a second by means of a DAQ. The registering of the real slip between both materials was impossible to carry out as the bar did not completely cross the specimens. Thus, the displacement values expressed included all the other external deformations such as slip in the clamps, neoprene compression, concrete deformation, free length steel bar deformation, etc. Consequently, the slip values obtained in Phase 1 and Phase 2 were not directly comparable. The τ_{max} being the only comparable data.

3.3 Accelerated corrosion

3.3.1 Corrosion method

Corrosion of steel reinforcement was induced by means of the passing of an electrical current. Following Faraday's law, Eq. 2, it is possible to determine the weight loss of steel at any given time through corrosion, due to the applied intensity of the electrical current I(t), together with the diameter and exposed length of bar.

$$\boldsymbol{E = \frac{m_{Fe} \cdot \int I \cdot dt}{V \cdot F}} \quad \textbf{(2)}$$

Where, m_{Fe} is the atomic mass, V is the steel Valencia that is equal to two and F is the Faraday's constant. As the applied intensity was a constant input during the whole duration of the test, it is possible to rewrite Faraday's law as Equation3, in order to determine the weight loss of steel.

$$\boldsymbol{\Delta m = \frac{m_{Fe} \cdot I \cdot t}{V \cdot F}} \quad \textbf{(3)}$$

Many researchers have claimed [38,39] that the use of current densities below 200 μA/cm^2 for accelerated corrosion tests causes a similar (5-10% difference) loss of weight in the steel to weight loss of bars estimated by Faraday's law.

Thus, it is possible to accurately estimate the corrosion degree achieved by applying electrical current density values below this threshold. Furthermore, current densities above this threshold cause earlier cracking as well as a notable difference with the real corrosion procedure and resulting corrosion products. It is known that the bond between steel and concrete is affected by the corrosion rate [40]. In the present work, 1% loss of weight of steel bar by corrosion procedure, at ten days was estimated and consequently 130 μA/cm^2

of electrical current density was applied. The same electrical current density was also maintained over a period of 20 and 30 days in order to produce 2% and 3% of weight loss of steel bar due to the corrosion procedure.

In order to produce accelerated corrosion of embedded steel bars by means of impressed current, the steel bars must be depassivated. As previously mentioned in this particular experimental study sodium chloride was added to the concrete mixing water in order to eliminate the passive layer by means of chloride attack.

3.3.2 Corrosion procedure

The specimens produced in Phase 2 were placed into plastic recipients and approximately 90% of their volume immersed (90 mm) in water, which contained 5% of NaCl solution (electrolyte). A copper plate was located under the concrete specimens, see Fig. 4. The copper plate was used as a cathode during the corrosion process, and the steel bar was used as anode. The steel bar and copper plate were connected to the power supply equipment, which provided the specified current as defined earlier. A different number of specimens was connected in series guaranteeing the same intensity (see Fig. 5).

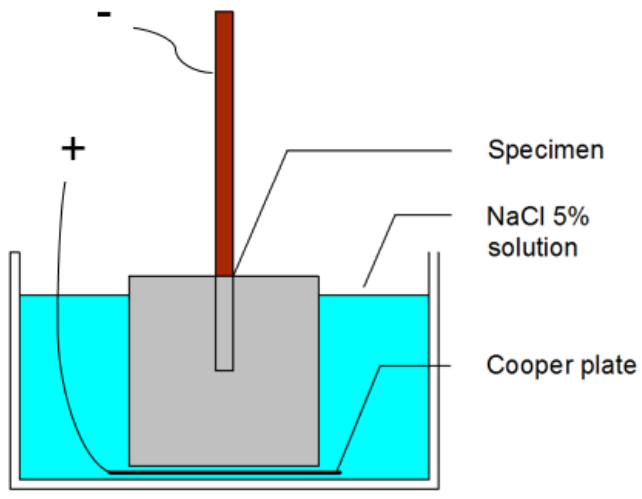

Fig. 4. Test setup induced corrosion

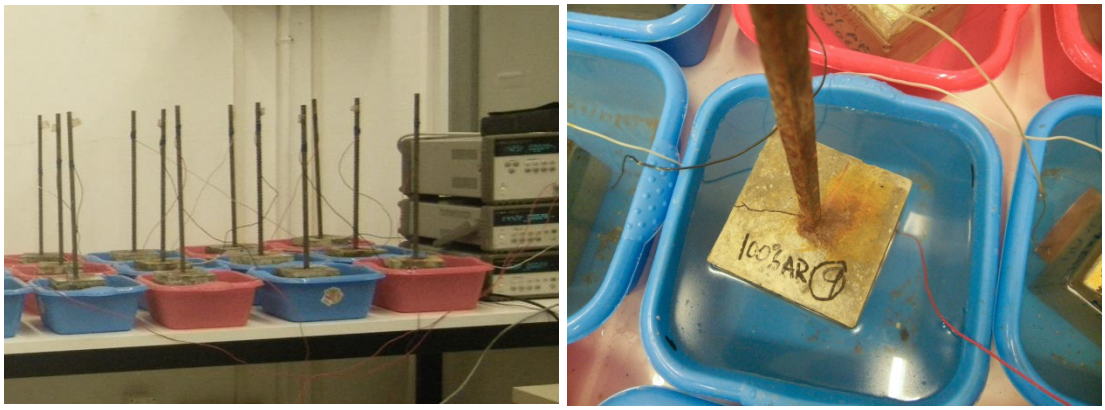

Fig. 5. Series connection scheme for corrosion procedure

The instant of the first cracking appearance on the surface of the different types of concrete specimens during corrosion process was evaluated.

Three specimens of each type of concrete (CC, RAC-20, RAC-50 and RAC-100) were exposed to the corrosion process at three different ages, 10 days (1% estimated corrosion degree by Faraday's law), 20 days (2% estimated corrosion degree by Faraday's law) and 30 days (3% estimated corrosion degree by Faraday's law). All the specimens were tested by employing the pull-out test described previously (Phase 2). The percentage of mass loss was measured and compared with the Faraday's law prediction, in each type of concrete. Chemical cleaning of corroded steel specimens was performed to calculate the steel mass loss, following the specifications [41]. The cleaning procedure was conducted using a solution of hydrochloric acid.

4. Test results

4.1 Concrete properties

Table 4 describes the compressive strength at 28 days of curing and the standard deviation of the values for all types of concretes produced.

Table 4. Compressive strength and experimental and theoretical Bond strength (τ_{max}) obtained in phase 1 and phase 2 uncorroded specimens for the four concretes cast

Concrete Type	Compressive strength (MPa)		τ_{max}-Pull Out test	
	Average	Std.	Phase1 Exp.	Phase2 Exp. (un.)
CC	51.2	0.92	28.64	34.36
RCA-20	48.28	0.66	29.69	35.78
RCA-50	47.8	0.21	27.14	32.57
RCA-100	49.95	3.05	30.31	35.63

As expected, there was no significant drop in the compressive strength of the RAC specimens with respect to that of CC concrete specimens, due to the adequate compressive strength (40MPa) of the parent concrete. The weak point of medium–high strength concretes made with coarse recycled concrete aggregates can be determined by the strength of the recycled concrete and its attached mortar [18,24]. According to Hansen and Narud [42] the compressive strength of recycled concrete is also strongly correlated with the water –cement ratio of the parent concrete. If the w/c ratio of the parent concrete is the same or lower than that of recycled concrete, the new strength of the recycled concrete will be as good as or better than that of original concrete.

In conventional concrete there is only one type of Interfacial Transition Zone (ITZ), i.e., between the natural aggregates and cement paste, while in recycled aggregate concretes there are in fact two: one between the recycled aggregates and the new cement paste and the other (inside recycled aggregate) between the original aggregate and the adhered mortar from the parent concrete. These frontier zones significantly condition the concrete's performance. The failure of recycled aggregate concrete produced employing low strength

RCA parent concretes occurs in the ITZ between the original aggregates and the adhered mortar or through the adhered mortar of RCA. Contrarily to what happens in recycled aggregate concrete mixed with recycled aggregates from medium-high strength parent concretes. Here the weakest zone is the ITZ between the aggregates (recycled or natural) and the new paste [43], and consequently the compressive strength is not influenced by the adhered mortar. According to Soares et al. [44] the compressive strength of recycled aggregates achieved identical compressive strength to that of conventional concrete, being justified by the shape of the aggregates , their adherence to the cement paste and the quality of the source concrete. Gonzalez and Etxeberria [45] also concluded that recycled aggregate concretes produced employing recycled aggregate from a 100 MPa parent concrete reached identical values to the conventional concrete (around 100 MPa), even for total aggregates' replacement. However, in all those cases [43-45] it was found that the modulus of elasticity was lower in the recycled aggregate concretes compared to CC concrete. The capacity of the aggregates to resist deformations is controlled by their stiffness and influenced by their porosity. The recycled aggregates are therefore more deformable because of the high porosity of the adhered cement paste.

4.2 Pull-out test results. Type of concrete influence

4.2.1 Pull-out test results: Phase 1

The results of direct pull-out test in terms of τ_{max} (maximum bond capacity) for the specimens produced at Phase 1 are shown in Table 4. As expected the failure mode described was splitting as a consequence of the obtained results of the compressive strength and the c/D ratios employed for the test setup. However, the remaining bond capacity did not drop to zero after the failure took place. The value of τ_{max} was very similar in all the

concretes with lower than 10% variation with respect to the maximum bond capacity of CC. That variation was in accordance with the compressive strength obtained by RAC and CC concretes, as already reported by other researchers [10,46].

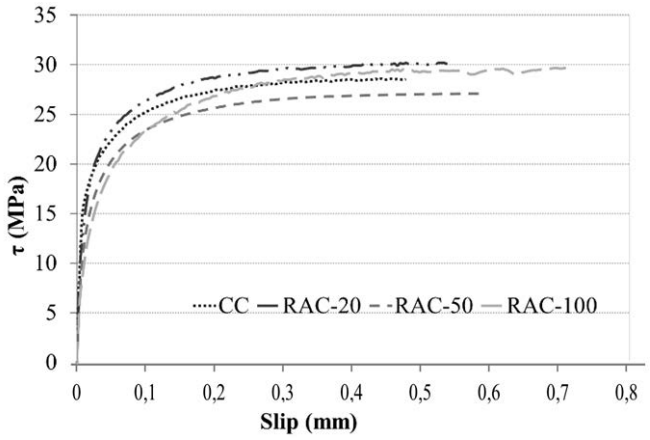

Fig. 6. Direct bond τ (MPa)-slip (mm) curves of the four types of concrete

The LVDT placed underneath the specimen was able to monitor and register the actual direct slip between the concrete and steel bar. Fig. 6 shows the direct bond-slip curves of the four types of concretes. It shows that the maximum slip registered was higher in RAC concretes, and it increased when higher percentages of recycled aggregates were used. Fig. 7 illustrates the pull-out test of CC concrete.

Fig. 7. Specimen after pull-out test

335 Fig. 8 shows the average values of the instant τ with respect to the τ_{max} ratio for each type
336 of concrete according to the instant slip respect to the $slip_{max}$ ratio. The CC, RCA-20, RCA-
337 50 concretes showed almost the same stiffness with smooth variations in the curves.
338 However, RCA-100 presented higher slips for the same τ_{max}. There was a considerable
339 reduction in stiffness, more than 30%, in the RAC-100 concrete when compared to other
340 concretes. A behaviour fact which has also been documented by other authors [14]. It is
341 also known that the modulus of elasticity is reduced with the employment of RCA for
342 concrete production [20,24] and it is coherent with the behaviour observed in Fig. 6 and 8.
343 The higher porosity registered for RCA concretes could correctly explain this behaviour in
344 concretes produced with 100% of RCA.

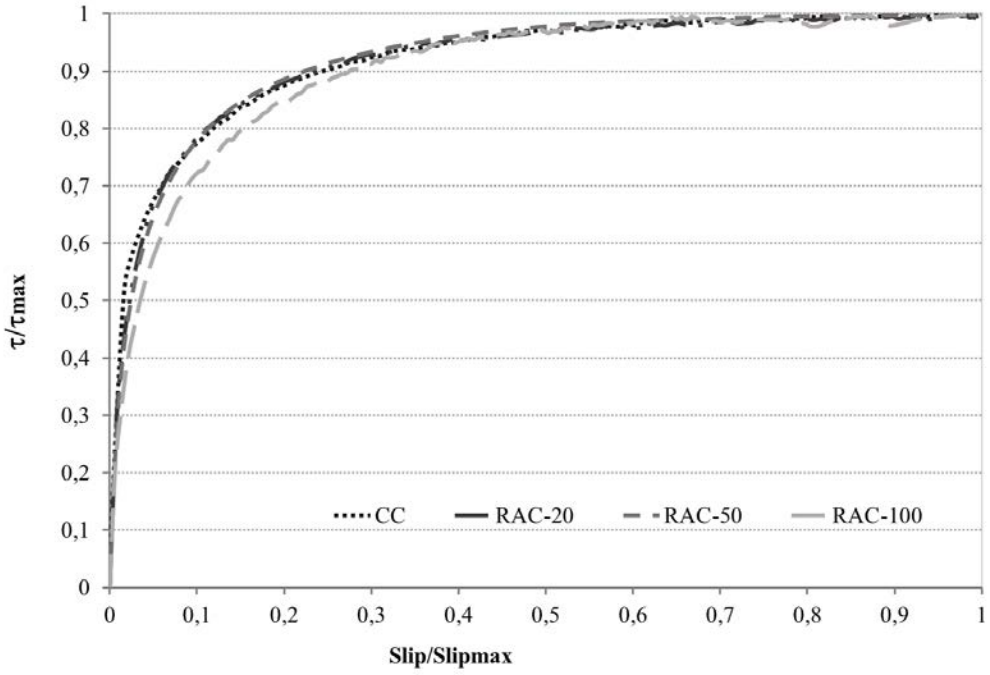

345

346 **Fig. 8. Unitary τ /τ_{max} respect to slip/$slip_{max}$ curves of the four types of concrete**

347

348 *4.2.2 Pull-out test results: Phase 2 (uncorroded)*

349 The τ_{max} value for the four types of concrete specimens, with uncorroded bars, are shown in
350 Table 4. The τ_{max} value for recycled aggregate concretes was similar to that obtained for
351 CC concrete. RAC-20 concrete presented a slightly higher τ_{max}, when RAC-50 suffered a
352 lower reduction than 10% with respect to the value of conventional concrete. The RCA-100
353 obtained a similar value to that of CC concrete. These values were in accordance with those
354 obtained in Phase 1 and also in accordance with similar compressive strength results
355 obtained by all the concretes. As mentioned by some researchers [47,48] the bond between
356 reinforcing steel and concrete depends on the geometric properties of both steel and
357 concrete as well as of the concrete properties. Regarding concrete properties, its
358 compressive strength is stated as the most important parameter. Kim and Yun [47]
359 confirmed that the compressive strength was also the adequate parameter to be used for
360 bond strength characterization for concretes produced employing fine recycled aggregates.

361 *4.2.3 Discussion*

362 Fig. 9 shows the ratio between the τ_{max} (Phase 1), τ_{max} (Phase 2) and the compressive
363 strength for the three RA concretes produced with respect to the same values of CC
364 concrete. As illustrated, the results obtained by recycled aggregate concretes were similar
365 to those obtained by conventional concrete. The τ_{max} value for recycled aggregate concretes
366 reached or exceeded that of conventional concretes except for the concrete produced with
367 50% of recycled aggregates. In all cases, all the registered variations were attributed to the
368 inherent high dispersion of the pull-out tests [37].

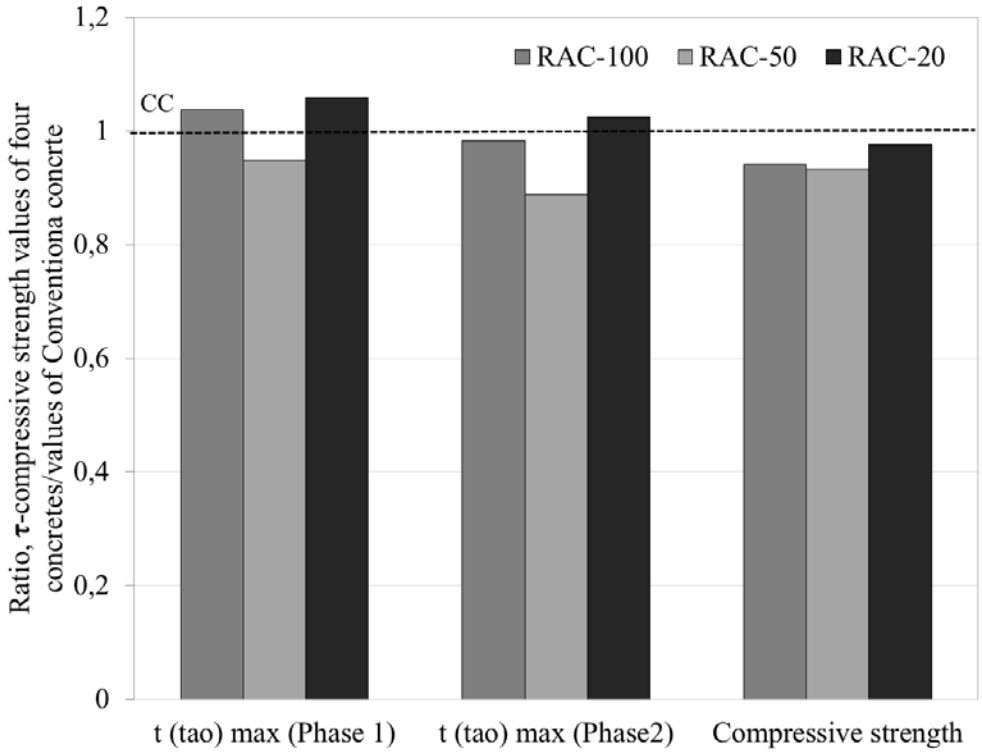

Fig. 9. Ratio of τ_{max} (phase 1), τ_{max} (phase2) and compressive strength of all the concrete produced with respect to the same values of conventional concrete.

Fig. 10 shows the influence of compressive strength on τ_{max} values, determined by the ratio of $\tau_{max\text{-}RAC}/\tau_{max\text{-}CC}$ with respect to $f_{c\text{-}RAC}/f_{c\text{-}CC}$. All the values were approximately one, due to the similar compressive strength of all the concretes studied and its influence on bond strength determination in any type of concretes. Similar conclusions were obtained by other researchers [47–49].

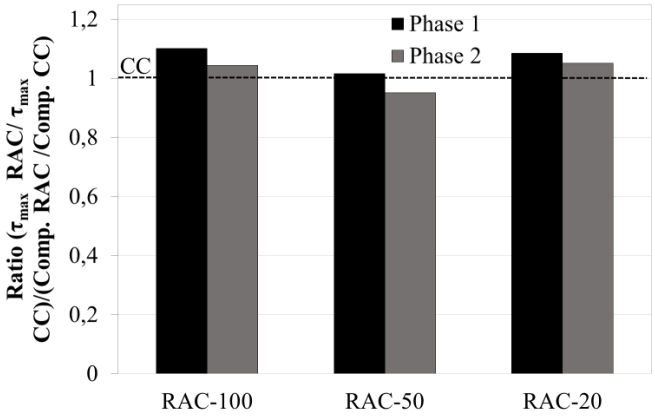

Fig. 10. Ratio of $\tau_{max\text{-}RAC}/\tau_{max\text{-}CC}$ with respect to $f_{c\text{-}RAC}/f_{c\text{-}CC}$.

4.3 Phase 2 results. Corrosion degree influence

4.3.1 Weight loss determination

Table 5 shows the resulting mass loss for each specimen and the average weight loss of all bars at different exposition time. The weight loss obtained experimentally was a little higher than that determined by Faraday's law at 10 day and 20 days of exposure. However, at 30 days of exposure the real mass loss was higher, probably due to the influence of concrete cracking in the accelerating of corrosion process. In any case as described in Maadaway et al. [38], experimental results of the accelerated corrosion method always produced higher mass loss than the theoretical estimation. Fig. 11 demonstrates the steel bars before and after the cleaning was performed.

393 Table 5. Determined corrosion levels by mass loss.

Type of concrete	10 exposition days (1% mass loss according to Faraday's law		20 exposition days (2% mass loss according to Faraday's law)		30 exposition days (3% mass loss according to Faraday's law)	
	Corrosion level (%)	Average (%)	Corrosion level (%)	Average (%)	Corrosion level (%)	Average (%)
CC	--	1.65	1.86	2.6	5.71	5.75
	--		1.89		6.59	
	--		2.18		5.65	
RAC-20	1.66		2.42		5.40	
	0.83		2.54		5.75	
	1.58		2.40		4.99	
			2.61			
RAC-50	1.35		3.16		5.94	
	1.86		2.24		6.65	
	1.93		3.28		5.02	
RAC-100	2.23		2.91		6.35	
	1.69		3.04		5.43	
	1.70		3.04		5.60	
			2.87			

394

Fig. 11. Steel bar specimens before and after cleaning procedure

4.3.2 Surface cracking due to corrosion procedure

Cracks produced by corrosion are a major problem during the concrete deterioration process. The instant of the first surface cracking of each type of concrete during the electrical current exposition period was determined (see Table 6).

Table 6. Description of the exact time of the first cracking of each type of concrete and the ratio of required time by each RAC concretes with respect to that of CC in percentage

Concrete type	CC	RAC-20	RAC-50	RAC-100
First cracking time (in days)	4.75	6.15	7.66	6.55
Ratio of required time (%)	0	29.47	61.26	37.89

It was noted that the RAC concrete needed approximately 30% more exposure time than conventional concrete for the first surface cracking to appear. According to Yalciner et al. [33] the concretes produced with high water/cement ratio needed more time for the first outer cracking than concretes with low water/cement ratio. This being due to the lower

409 porosity of later ones. The high porosity of concrete had similar adequate influence on the
410 occurrence of the first cracking in all tested concretes. In this research work the higher
411 porosity of the recycled aggregates, which had a greater capacity for absorbing the internal
412 stresses caused by the corrosion products, delayed the surface cracking. A higher corrosion
413 degree was needed in order to achieve the same external cracking for RAC.

414 Table 7. Description of surface cracking pattern caused by corrosion cracking

Concrete type	Estimated corrosion level	External Crack amount	Numeration of cracks on upper face (cms)			Numeration of Crack on lateral faces (cms)			τ_{max} (MPa)
			1	**2**	**3**	**1**	**2**	**3**	
CC	1%	3	6.0	5.0	4.5	-	3.0	5.5	5.53
		3	3.0	5.0	5.0	-	4.0	6.5	5.47
	2%	3	6.0	5.0	4.5	-	3.0	5.5	4.09
		3	3.0	5.0	5.0	-	4.0	6.5	5.37
	3%	2	4.5	4.5	-	8.0	9.0	-	3.47
		2	4.0	4.5	-	9.0	8.5	-	4.13
		3	4.0	4.5	4.0	10.0	8.5	5.5	4.39
RAC-20	1%	3	2.5	5.5	4.5	-	-	2.0	6.72
		2	4.4	4.5	-	1.0	5.5	-	7.13
	2%	2	4.0	4.5		7.0	5.0		6.61
		3	5.0	4.5	5.0	5.0	6.5	7.0	4.92
		3	6.0	5.0	4.0	4.5	3.5	8.0	5.28
		2	4.5	4.5	-	4.0	7.0	-	5.81
	3%	2	5.0	4.0	-	7.5	3.0	-	5.31
		2	5.0	4.5	-	5.5	6.0	-	4.32
RAC-50	1%	1	7.0	-	-	-	-	-	6.91
		2	4.0	4.0	-	1.5	6.0	-	6.24
	2%	3	4.0	5.5	6.0	4.0	5.0	-	5.20
		3	4.5	4.5	4.0	8.0	1.0	9.5	5.65
		3	5.0	4.5	5.0	8.0	8.0	6.0	6.30
	3%	1	5.5	-	-	6.0	-	-	5.04
		1	4.5	-	-	8.5	-	-	3.53
RAC-100	1%	3	4.7	4.0	4.0	-	-	-	8.40
		2	5.5	4.0	-	5.5	5.5	-	7.67
	2%	3	4.0	4.5	5.0	3.0	8.0	4.5	6.58
		3	4.2	5.5	4.0	1.0	4.0	4.5	6.30
		3	6.0	5.5	4.5	4.5	6.5	8.0	5.49
	3%	2	4.5	4.5	-	7.0	9.0	-	3.90
		3	4.0	6.5	6.0	8.5	6.0	6.0	4.50

415

A description of surface crack pattern caused by corrosion cracking is described in Table 7 (Fig. 12 illustrates the cracking of CC and RAC-100 at 1.6% and 5.75% of corrosion degree). The first outer cracks appeared on the upper face of the concrete cubic specimens, in which the steel bar was embedded. The cracks became prolonged on the lateral faces due to the increase of corrosion degree. Table 7 describes the total amount of cracks that appeared: the enumeration of the upper face cracks represents the order of occurrence, whilst the lateral face crack's enumeration corresponds to the number of the upper face crack prolongation. The τ_{max} of all the corroded samples is also described in the same Table 7.

(a) CC concrete at 1.6% corrosion degree

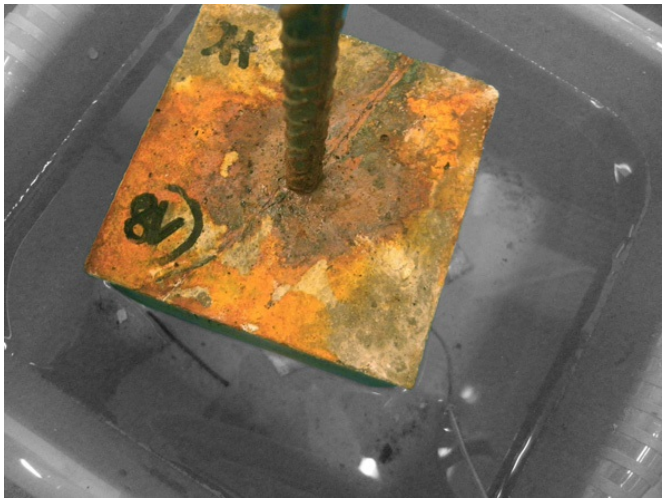

(b) CC concrete at 5.75% corrosion degree

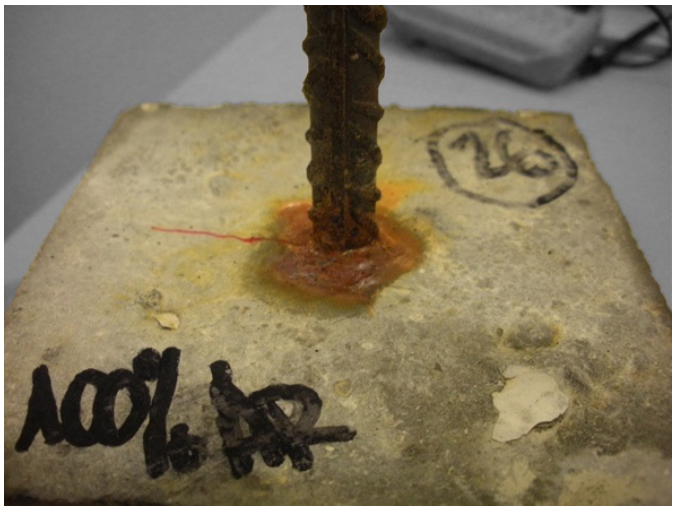

(c) RAC-100 concrete at 1.6% corrosion degree

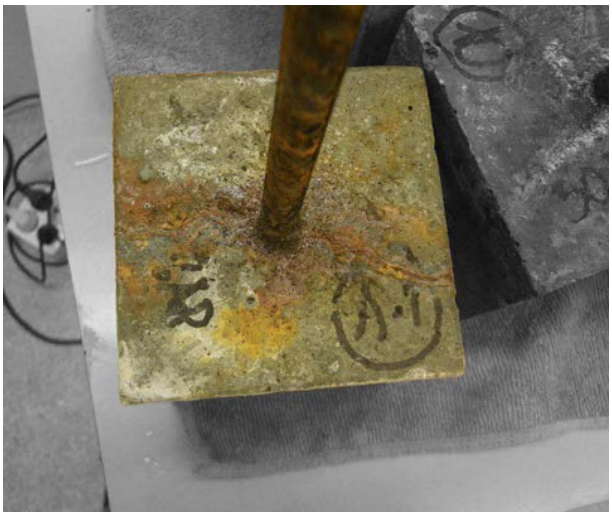

(d) RAC-100 concrete at 5.75% corrosion degree

Fig. 12. Cracking of different specimens after corrosion exposition

It must be considered as remarkable that there was no clear relationship between the values obtained by the visual crack measurements and the τ_{max} achieved for each concrete by means of the direct pull-out tests (Phase 2). A similar behaviour was stated by Yalciner et al. [33], where the bond strength capacity was not attributed to the number of cracks in conventional concretes. That phenomenon could most probably be attributed to the different internal damage on each specimen. Due to the impossibility of observing the internal damage via a visual inspection a post pull-out test examination was performed on the samples.

Fig. 13. Surface cracking of RAC-50 at 5.75% of corrosión degree.

Nearly all the samples showed 2 or 3 upper surface cracks which later became prolonged on the lateral faces. However, with respect to the RAC-50 concrete it was noted that after 30 days of being induced by electrical current (of 130 μA/cm^2) it only suffered one crack on its upper surface, which later became prolonged on one of the lateral faces (see Fig. 13). However, in accordance with the above-mentioned hypothesis, the pull-out test revealed severe internal damage. The corrosion products could fill the pores of concrete producing stress and changing the crack pattern. Consequently, specimens could not release those products causing internal damage. Fig. 14 depicts other specimens with differing forms of internal damage, revealing different internal crack formations.

Fig. 14. Internal damage cracking for RAC-50

4.3.3 Corrosion degree influence on bond-slip relationships

Table 8 describes the results of the pull-out tests (τ_{max} and its standard deviation) carried out with uncorroded (0% corrosion degree) and corroded steel bars (with 1.6%, 2.6% and 5.75% corrosion degree). As previously mentioned, CC concrete and RAC concretes had similar bond strength when they were not exposed to the corrosion effect.

At the different degrees of the steel bar corrosion (1.65%, 2.60% and 5.75%), the bond strength for all RAC specimens was higher than that of the CC concrete. In addition, this difference increased when a larger amount of RCA was employed in concrete production. Consequently, the concretes produced with a large amount of RCA presented better behaviour in terms of bond capacity under corrosion. Nevertheless, this better response significantly decreased as the specimen became more corroded, achieving roughly similar τ_{max} values after 5.75% of degree of corrosion.

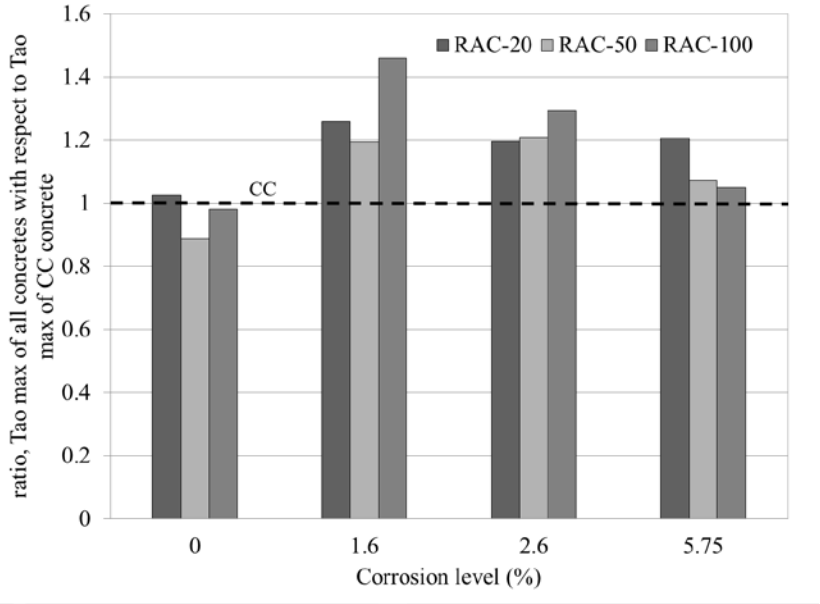

Fig. 15. Ratio of τ_{max} (phase2) of all the concrete produced with respect to that value of conventional concrete at different corrosion degree (%) .

Fig. 15 shows the ratio of the τ_{max} of the recycled aggregate concretes with respect to that of the conventional concrete at different corrosion degrees. It can be observed that the τ_{max} was higher in all of the RAC concretes than in the CC, independent of the percentages of recycled aggregates used for concrete production and the corrosion degree of the steel bars.

Although an improvement of the bond capacity in RAC was observed at all the tested corrosion levels, that improvement was found to be almost negligible for higher corrosion levels.

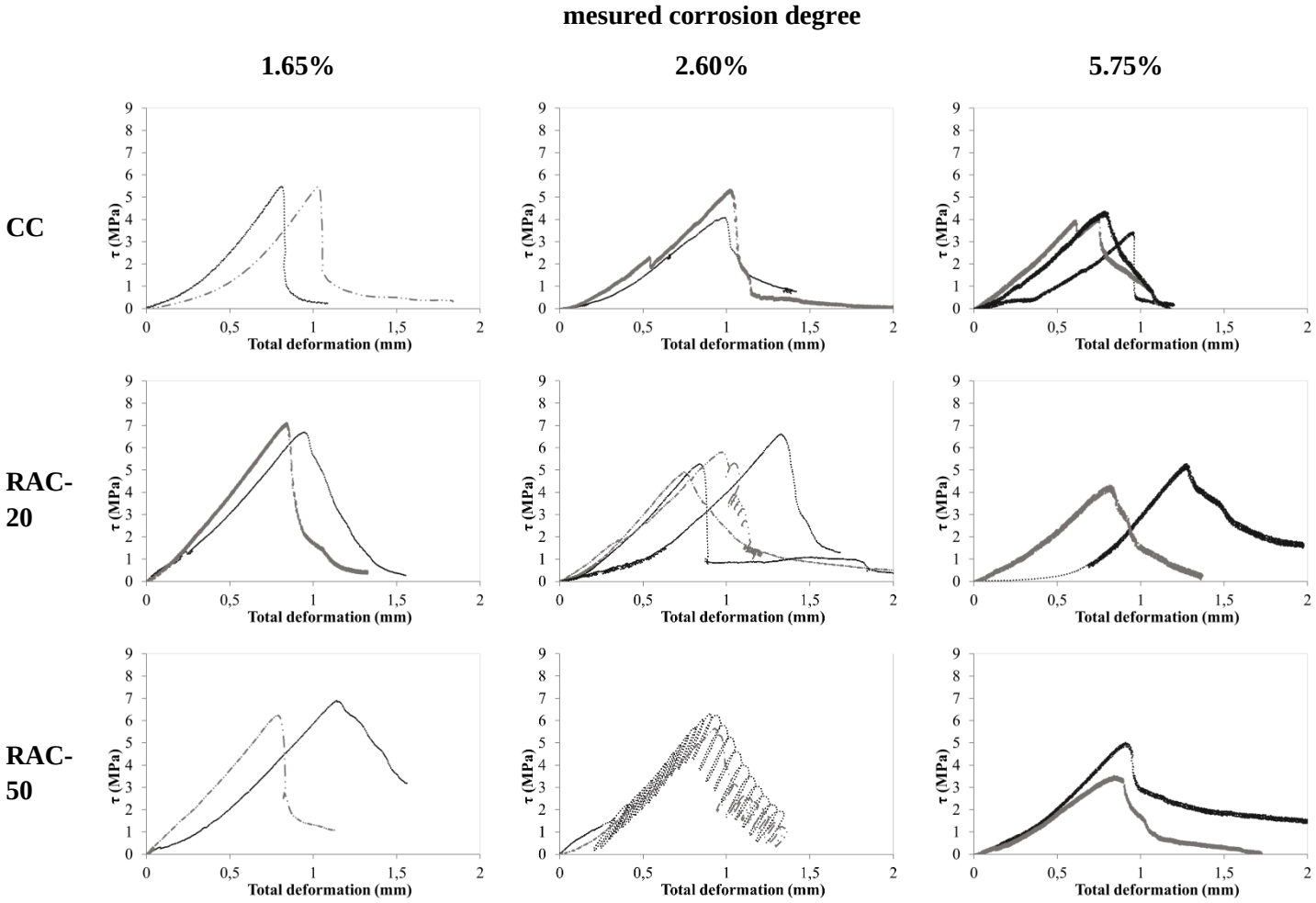

RAC-100

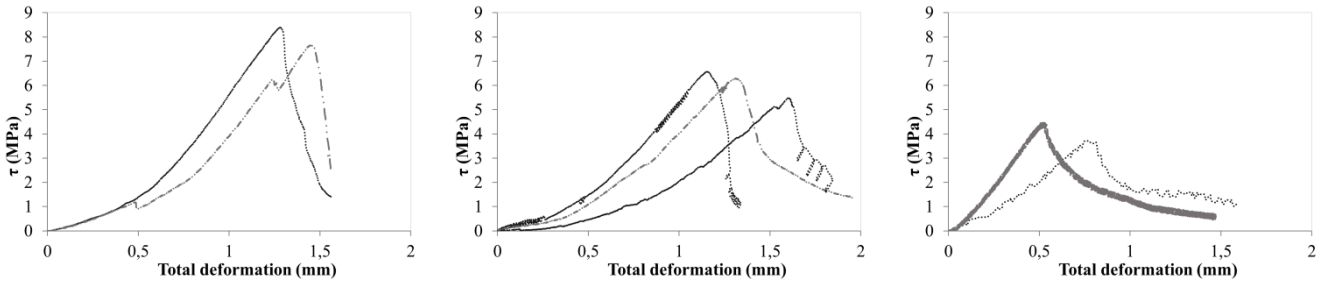

Fig. 16. Bond (τ, MPa) –displacement (mm) behaviour of all the tested corroded specimens

Fig. 16 describes the bond-displacement behaviour of all the tested corroded specimens (2-4 samples were used in each type of concretes). As mentioned, the displacement showed corresponds to a total displacement which includes slip in the clamps, free steel bar length deformation, etc., as well as the slip between both materials. This is due to the configuration of the pull-out test in Phase 2. However, it is possible to observe the specimen's general behaviour in terms of τ-displacement**.** The concretes produced employing a higher amount of RCA suffered a higher total deformation, in accordance with the results described in Phase 1, where the RCA-100 showed a stiffer bond-slip behaviour than the other specimens.

The increase of the bond strength of the RAC concrete occurred while there was a very low degree of corrosion. This was probably due to the confinement effect cause by the expanded corrosion product between bars and concrete. According to other researchers [49–51] slight corrosion of the steel improves the bond strength due to the increase in steel bar surface roughness or friction. Furthermore, the higher porosity of CC concrete [33] and consequently of RAC reduced the stress level in the surrounding concrete (due to its absorption capacity of that product) increasing the bond strength. However, for high

corrosion degrees, the absorption capacity of those concretes has no influence on the cause of a significant bond strength reduction as was described in this study.

4.4 Ultimate bond strength (τ_{max}) estimation models

There are few mathematical models in the literature upon the subject which estimate/ predict the bond strength value for CC [33,52] and as expected much fewer models designed to determine the bond strength for RAC concretes [11,13].

In accordance with the bond strength prediction of CC concrete, the values obtained by Model Code [52] depend on the compressive strength of the concrete. The model defined by Yalciner et al. [33] takes into account the compressive strength of concrete and the ratio between the concrete cover and steel bar diameter for the pull-out test setup. The model defined by Kim &Yun [11] for RAC concretes, takes into account the compressive strength of conventional concrete, the ratio between the concrete cover and steel bar diameter for pull-out test setup and the influence of a percentage of RCA in the concrete.

Fig. 17 shows the estimated bond strength values of the four types of concretes according to the three mathematical models described previously, defined by Kim &Yun [11], Model Code [52], and the model defined by Yalciner et al. [33]. The bond strength values predicted by Kim & Yun model [9] underestimated the real experimental values obtained by recycled aggregates concretes as it considers the compressive strength of RAC to be lower than that of conventional concrete due to the presence of RCA which consequently also effects the bond strength.

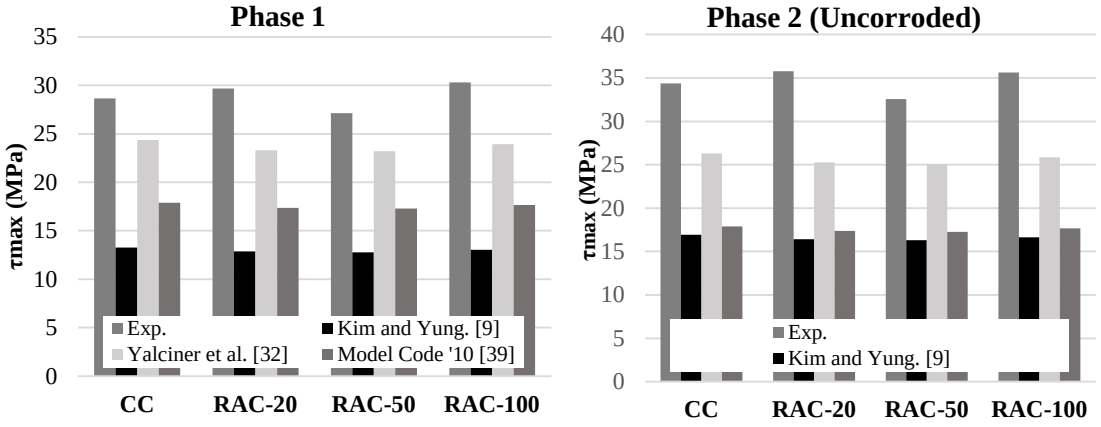

Fig. 17. Phase 1 and Phase 2 experimental and numerical bond strength values.

However, of all three model, the model defined by Yalciner et al. [33], predicts more adequately the bond strength of all the concretes. It considers that the prediction of the bond strength of any concrete depends only on its compressive strength values and the ratio between the concrete cover and steel bar diameter for the pull-out test. It does not take into account the influence of a different percentage of RCA. The models defined for the prediction of the bond strength of CC concretes could be employed to adequately predict the bond strength of recycled aggregate concrete when those RAC concretes are produced with the similar compressive strength of the parent concrete of RCA. The Model Code [52] underestimated the bond strength of both types of RAC and CC concretes as it only considered the compressive strength of concrete as input.

Yalciner et al. [32] proposed an analytical model for the determining of bond strenth between concrete and the different degrees of corroded reinforcing steel. That model could be employed when the ratio cover/diameter (c/D) is between 1 and 3.2. It must be noted that the ratio c/D for the tested specimens is 4.5, which is outside the bounds defined in the model. Fig. 18 shows the obtained results in this research work in comparison to the

values calculated by the mentioned model. According to the obtained results, the model overestimated the results achieved by the four types of concretes at low corrosion degrees except for concretes produced employing 100% of recycled aggregates, which was adequately predicted at low degrees of corrosion. The model also adequately predicted the behaviour of all the concretes at 5.75% corrosion degree. The trend described for both the experimental data and the numerical data was very similar. However, the real behaviour showed a pronounced drop in bond capacity for lower degrees of corrosion.

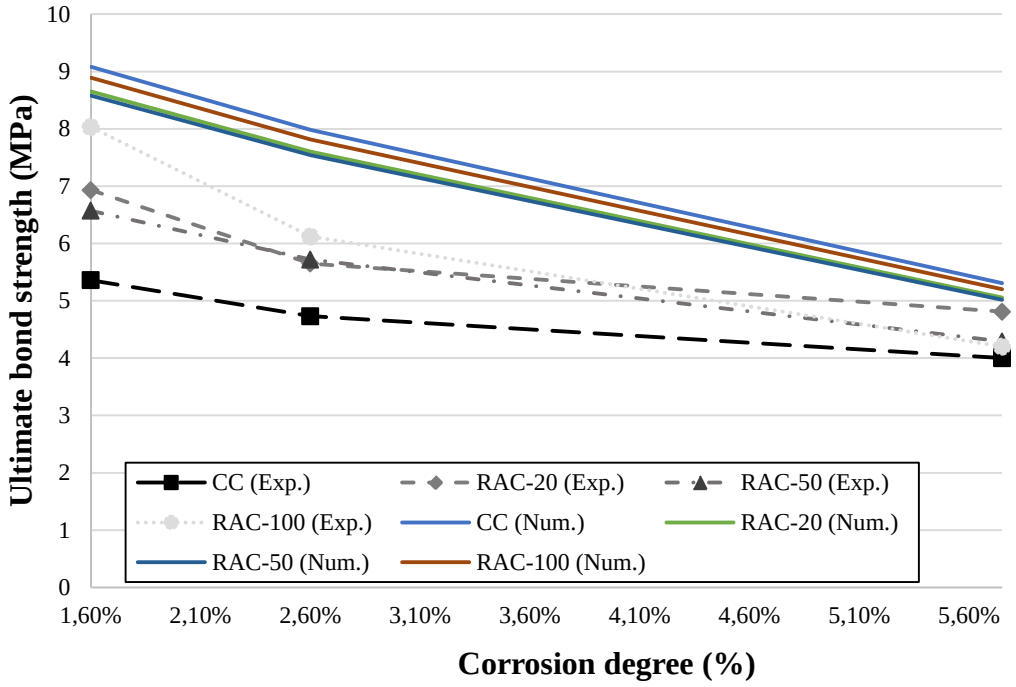

Figure 18. Experimental and numeral bond strength values for corroded specimens.

5. Conclusions

Based on the results of the study, the following conclusions can be drawn:

(1) The bond behaviour is strongly dependent on compressive strength values. The recycled aggregate concretes which had a similar compressive strength to that of conventional concrete obtained similar or better bond strength.

(2) Recycled aggregate concretes produced employing up to 50% of coarse recycled aggregates achieved similar slip and bond strength to those of conventional concrete. However, the recycled aggregate concrete produced with 100% of RCA suffered a substantial stiffness drop.

(3) On reaching the same degree of corrosion, it was noted that the initial cracking (visually detectable) of recycled aggregate concretes occurred later than in conventional concrete. Furthermore, there is no determined relationship between the amount of cracks produced with RA replacement and the corrosion degree, nor is there a relationship between the amount of cracks and maximum bond strength.

(4) The employment of a higher amount of RCA leads to better bond strength performance at very low degrees of corrosion due to the higher porosity of the recycled concrete aggregates which also leads to a bond improvement. Higher degrees of corrosion caused similar behaviour on RAC and CC concretes.

(5) The increase of the corrosion damage propagation phase in the structural service life of RAC concrete takes place due to its capacity to reduce longitudinal cracking and development of better bond strength performance for low degrees of corrosion.

(6) The ultimate bond strength estimation models used for CC were adequate for the prediction of the bond strength of the RAC, when the compressive strength of the

RCA parent concrete was found to be similar or higher to that of RAC. In order to validate an ultimate bond strength, one must take into consideration, not only its compressive strength and the percentage of RCA, but also parameters such as ratio cover/diameter and the compressive strength of RCA parent concrete. The model presented by Yalciner et al. [33] amply described quite well the bond behaviour of the corroded specimen. However, a calibration with a more extended database is needed in order to adjust the real observed behaviour accurately.

It would be advantageous to produce a further work based on an analysis of wider ranges of degrees of corrosion using slower corrosion rates. The resulting values obtained from RAC, which would have been subjected to corrosion over extended periods of time and consequently simulating a more natural corrosion procedure, are expected to be defined as behaving even better than those obtained in this research work. This improvement in behaviour consequently resulting in better adequate propertie with respect to that of CC concrete.

Acknowledge

The authors wish to acknowledge the financial support of The Ministry of Economy and Competitiveness of the Government of Spain (MINECO) for providing funds for projects BIA2009-11764 as well as INNPACT project (IPT-2012-1093-310000) and the European Regional Development Fund (FEDER). The financial support of Infrastructures de Catalunya (ICAT) for personnel expenses is also highly appreciated.

582 **References**

583 [1] K.Z. Hanjari, K. Lundgren, D. Coronelli, Bond capacity of severely corroded bars
584 with corroded stirrups, Mag. Concr. Res. 63 (2011) 953–968.
585 doi:10.1680/macr.10.00200.

586 [2] I. Sæther, Bond deterioration of corroded steel bars in concrete, Struct. Infrastruct.
587 Eng. 7 (2011) 415–429. doi:10.1080/15732470802674836.

588 [3] D. Coronelli, K.Z. Hanjari, K. Lundgren, Severely Corroded RC with Cover
589 Cracking, J. Struct. Eng. 139 (2013) 221–232. doi:10.1061/(ASCE)ST.1943-
590 541X.0000633.

591 [4] A. Muñoz Noval, C. Andrade, A. Torres, J. Rodríguez, Relation between Crack
592 Width and Diameter of Rebar Loss Due to Corrosion of Reinforced Concrete
593 Members, ECS Trans. 3 (2007) 29–36. doi:10.1149/1.2721428.

594 [5] C. Alonso, C. Andrade, J. Rodriguez, J.M. Diez, Factors controlling cracking of
595 concrete affected by reinforcement corrosion, Mater. Struct. 31 (1998) 435–441.
596 doi:10.1007/BF02480466.

597 [6] K. Lundgren, P. Kettil, K.Z. Hanjari, H. Schlune, A.S.S. Roman, Analytical model
598 for the bond-slip behaviour of corroded ribbed reinforcement, Struct. Infrastruct.
599 Eng. 8 (2012) 157–169. doi:10.1080/15732470903446993.

600 [7] K. Zandi Hanjari, K. Lundgren, M. Plos, D. Coronelli, Three-dimensional modelling
601 of structural effects of corroding steel reinforcement in concrete, Struct. Infrastruct.
602 Eng. (2011) 1–17. doi:10.1080/15732479.2011.607830.

603 [8] C. Fang, K. Lundgren, M. Plos, K. Gylltoft, Bond behaviour of corroded reinforcing
604 steel bars in concrete, Cem. Concr. Res. 36 (2006) 1931–1938.
605 doi:10.1016/j.cemconres.2006.05.008.

606 [9] M.R. Salari, E. Spacone, Finite element formulations of one-dimensional elements
607 with bond-slip, Eng. Struct. 23 (2001) 815–826. doi:10.1016/S0141-0296(00)00094-
608 8.

609 [10] J. Xiao, H. Falkner, Bond behaviour between recycled aggregate concrete and steel
610 rebars, Constr. Build. Mater. 21 (2007) 395–401.
611 doi:10.1016/j.conbuildmat.2005.08.008.

612 [11] S.-W. Kim, H.-D. Yun, Evaluation of the bond behavior of steel reinforcing bars in
613 recycled fine aggregate concrete, Cem. Concr. Compos. 46 (2014) 8–18.
614 doi:10.1016/j.cemconcomp.2013.10.013.

615 [12] S.-W. Kim, H.-D. Yun, Influence of recycled coarse aggregates on the bond behavior
616 of deformed bars in concrete, Eng. Struct. 48 (2013) 133–143.
617 doi:10.1016/j.engstruct.2012.10.009.

618 [13] S. Seara-Paz, B. González-Fonteboa, J. Eiras-López, M.F. Herrador, Bond behavior
619 between steel reinforcement and recycled concrete, Mater. Struct. 47 (2013) 323–
620 334. doi:10.1617/s11527-013-0063-z.

621 [14] I. Eiras López, J., Seara Paz, S., González Taboada, I., Vieito Raña,
622 COMPORTAMIENTO ADHERENTE EN HORMIGÓN CON ÁRIDO, in:

623 Comport. Adherente En Hormigón Con Árido Reciclado. Curva Tensión Adherente-
624 Deslizamiento, ACHE - Asociación cientificotécnica del hormigón estructural,
625 Madrid, 2014: pp. 1–10.

626 [15] FiB Bulletin 10 - Bond of reinforcement in concrete, 2000.

627 [16] L. Butler, J.S. West, S.L. Tighe, The effect of recycled concrete aggregate properties
628 on the bond strength between RCA concrete and steel reinforcement, Cem. Concr.
629 Res. 41 (2011) 1037–1049. doi:10.1016/j.cemconres.2011.06.004.

630 [17] Y. Zhao, H. Lin, K. Wu, W. Jin, Bond behaviour of normal/recycled concrete and
631 corroded steel bars, Constr. Build. Mater. 48 (2013) 348–359.
632 doi:10.1016/j.conbuildmat.2013.06.091.

633 [18] S.W. Tabsh, A.S. Abdelfatah, Influence of recycled concrete aggregates on strength
634 properties of concrete, Constr. Build. Mater. 23 (2009) 1163–1167.
635 doi:10.1016/j.conbuildmat.2008.06.007.

636 [19] T. Hansen, Recycled aggregate and recycled aggregate concrete, Second State-of-
637 the-art Report developments 1945–1985, Mater. Struct. RILEM. 111 (1986).

638 [20] T. Hansen, RILEM: recycling of demolished concrete and masonry, Report of
639 Technical Comité 37-DRC: Demolition and Reuse of Concrete, London, 1992.

640 [21] M.C. Limbachiya, T. Leelawat, R.K. Dhir, Use of recycled concrete aggregate in
641 high-strength concrete, Mater. Struct. 33 (2000) 574–580. doi:10.1007/BF02480538.

642 [22] K.K. Sagoe-Crentsil, T. Brown, A.H. Taylor, Performance of concrete made with
643 commercially produced coarse recycled concrete aggregate, Cem. Concr. Res. 31
644 (2001) 707–712.
645 http://www.sciencedirect.com/science/article/pii/S0008884600004762 (accessed
646 October 16, 2014).

647 [23] C.S. Poon, Z.H. Shui, L. Lam, H. Fok, S.C. Kou, Influence of moisture states of
648 natural and recycled aggregates on the slump and compressive strength of concrete,
649 Cem. Concr. Res. 34 (2004) 31–36. doi:10.1016/S0008-8846(03)00186-8.

650 [24] M. Etxeberria, E. Vázquez, A. Marí, M. Barra, Influence of amount of recycled
651 coarse aggregates and production process on properties of recycled aggregate
652 concrete, Cem. Concr. Res. 37 (2007) 735–742.
653 http://www.sciencedirect.com/science/article/pii/S0008884607000415 (accessed
654 May 26, 2014).

655 [25] R.V. Silva, J. de Brito, R.K. Dhir, Properties and composition of recycled aggregates
656 from construction and demolition waste suitable for concrete production, Constr.
657 Build. Mater. 65 (2014) 201–217.
658 http://www.sciencedirect.com/science/article/pii/S0950061814004437 (accessed
659 August 29, 2014).

660 [26] C.. Poon, Z.. Shui, L. Lam, Effect of microstructure of ITZ on compressive strength
661 of concrete prepared with recycled aggregates, Constr. Build. Mater. 18 (2004) 461–
662 468. http://www.sciencedirect.com/science/article/pii/S0950061804000388
663 (accessed May 29, 2014).

664 [27] M. Barra, E. Vázquez, Properties of concrete with recycled aggregates: influence of

properties of the aggregates and their interpretation., in: Proceeding Int. Symp. Sustain. Constr. Use Recycl. Concr. Aggreg., London, 1998: pp. 19–30.

[28] A. Ajdukiewicz, A. Kliszczewicz, Influence of recycled aggregates on mechanical properties of HS/HPC, Cem. Concr. Compos. 24 (2002) 269–279. http://www.sciencedirect.com/science/article/pii/S0958946501000129 (accessed October 24, 2014).

[29] J.R. Jiménez, J. Ayuso, A.P. Galvín, M. López, F. Agrela, Use of mixed recycled aggregates with a low embodied energy from non-selected CDW in unpaved rural roads, Constr. Build. Mater. 34 (2012) 34–43. http://www.sciencedirect.com/science/article/pii/S0950061812001195 (accessed October 28, 2014).

[30] J. a. Pérez-Benedicto, M. Del Río-Merino, J.L. Peralta-Canudo, M. De la Rosa-La Mata, Características mecánicas de hormigones con áridos reciclados procedentes de los rechazos en prefabricación, Mater. Construcción. 62 (2011) 25–37. doi:10.3989/mc.2011.62110.

[31] V. Corinaldesi, G. Moriconi, Influence of mineral additions on the performance of 100% recycled aggregate concrete, Constr. Build. Mater. 23 (2009) 2869–2876. http://www.sciencedirect.com/science/article/pii/S0950061809000713 (accessed October 7, 2014).

[32] F.M. de Almeida Filho, M.K. El Debs, A.L.H.C. El Debs, Bond-slip behavior of self-compacting concrete and vibrated concrete using pull-out and beam tests, Mater. Struct. 41 (2007) 1073–1089. doi:10.1617/s11527-007-9307-0.

[33] H. Yalciner, O. Eren, S. Sensoy, An experimental study on the bond strength between reinforcement bars and concrete as a function of concrete cover, strength and corrosion level, Cem. Concr. Res. 42 (2012) 643–655. doi:10.1016/j.cemconres.2012.01.003.

[34] Instrucción de hormigón estructural - EHE-08, 2008.

[35] A. Losberg, Cracks in continuous concrete road slabs and other concrete structures locked against movements from temperature and shrinkage, 1962.

[36] M.F. Ruiz, A. Muttoni, P.G. Gambarova, Analytical Modeling of the Pre- and Postyield Behavior of Bond in Reinforced Concrete, (2007) 1364–1372.

[37] N.E. UNE, UNE-EN_10080=2006, (2006).

[38] T.E.A. El Maaddawy, K.K.A. Soudki, Effectiveness of impressed current technique to simulate corrosion of steel reinforcement in concrete, J. Mater. Civ. …. (2003) 41–47. http://ascelibrary.org/doi/abs/10.1061/(ASCE)0899-1561(2003)15:1(41) (accessed July 3, 2014).

[39] M. Badawi, K. Soudki, Control of Corrosion-Induced Damage in Reinforced Concrete Beams Using Carbon Fiber-Reinforced Polymer Laminates, J. Compos. Constr. 9 (2005) 195–201. doi:10.1061/(ASCE)1090-0268(2005)9:2(195).

[40] M. Saifullah, L.L.A. Clark, M. Sailfullah, L.L.A. Clark, Effect of Corrosion Rate on the Bond Strength of Corroded Reinforcement, in: S.A. Press (Ed.), Proc. Int. Conf. Corros. Corros. Prot. Steel Concr., University of Sheffield, 1994: pp. 591–600.

[41] ASTM Standard G1, Standard practice for preparing, cleaning, and evaluating corrosion test specimens, (2011).

[42] T.C.H. and H. Narud, Strength of Recycled Concrete Made From Crushed Concrete Coarse Aggregate, Concr. Int. 5 (n.d.).

[43] D. Pedro, J. de Brito, L. Evangelista, Influence of the use of recycled concrete aggregates from different sources on structural concrete, Constr. Build. Mater. 71 (2014) 141–151. doi:10.1016/j.conbuildmat.2014.08.030.

[44] D. Soares, J. de Brito, J. Ferreira, J. Pacheco, Use of coarse recycled aggregates from precast concrete rejects: Mechanical and durability performance, Constr. Build. Mater. 71 (2014) 263–272. doi:10.1016/j.conbuildmat.2014.08.034.

[45] G. Andreu, E. Miren, Experimental analysis of properties of high performance recycled aggregate concrete, Constr. Build. Mater. 52 (2014) 227–235. doi:10.1016/j.conbuildmat.2013.11.054.

[46] S.-W. Kim, H.-D. Yun, Influence of recycled coarse aggregates on the bond behavior of deformed bars in concrete, Eng. Struct. 48 (2013) 133–143. doi:10.1016/j.engstruct.2012.10.009.

[47] S.-W. Kim, H.-D. Yun, Evaluation of the bond behavior of steel reinforcing bars in recycled fine aggregate concrete, Cem. Concr. Compos. 46 (2014) 8–18. doi:10.1016/j.cemconcomp.2013.10.013.

[48] Z. Dahou, Z. Mehdi Sbartaï, A. Castel, F. Ghomari, Artificial neural network model for steel–concrete bond prediction, Eng. Struct. 31 (2009) 1724–1733. http://www.sciencedirect.com/science/article/pii/S0141029609000789 (accessed March 23, 2015).

[49] Y.S. Choi, S.-T. Yi, M.Y. Kim, W.Y. Jung, E.I. Yang, Effect of corrosion method of the reinforcing bar on bond characteristics in reinforced concrete specimens, Constr. Build. Mater. 54 (2014) 180–189. http://www.sciencedirect.com/science/article/pii/S0950061813012221 (accessed March 23, 2015).

[50] L. Abosrra, A.F. Ashour, M. Youseffi, Corrosion of steel reinforcement in concrete of different compressive strengths, Constr. Build. Mater. 25 (2011) 3915–3925. http://www.sciencedirect.com/science/article/pii/S0950061811001632 (accessed February 13, 2015).

[51] Y. Zhao, J. Dong, Y. Wu, H. Wang, X. Li, Q. Xu, Steel corrosion and corrosion-induced cracking in recycled aggregate concrete, Corros. Sci. 85 (2014) 241–250. http://www.sciencedirect.com/science/article/pii/S0010938X14001991 (accessed November 25, 2014).

[52] Model Code 2010-Final draft, The international federation for structural concrete, FIB. Bulletin No 52 Fib, 2; Lausanne, 2012.